Enhanced viral production and infection of bacterioplankton during an iron-induced phytoplankton bloom in the Southern Ocean

Markus G. Weinbauer,[a,b,*] Jesus-Maria Arrieta,[b,c] Christian Griebler,[d] and Gerhard J. Herndl[b,e]

[a] CNRS, Laboratoire d'Océanographie de Villefranche, France; Université Pierre et Marie Curie-Paris6, Laboratoire d'Océanographie de Villefranche, France

[b] Department of Biological Oceanography, Royal Netherlands Institute for Sea Research (NIOZ), Texel, The Netherlands

[c] Instituto Mediterráneo de Estudios Avanzados (IMEDEA), CSIC-UIB, Esporles, Mallorca, Spain

[d] Institute of Groundwater Ecology, Helmholtz Center Munich, German Research Center for Environmental Health, Neuherberg, Germany

[e] Department of Marine Biology, University of Vienna, Vienna, Austria

Abstract

We followed the viral response to Fe-enrichment over 3 weeks during the second iron-enrichment experiment (EisenEx) in the Southern Ocean. Although viral abundance increased in a rather constant way during the course of the experiment inside the patch, the production of bacterial viruses and the fraction of infected cells in bacterioplankton exhibited pronounced maxima on days 7 and 21. In contrast, these parameters remained fairly constant outside the Fe-fertilized patch. Viral production was also stimulated directly after the Fe-enrichment. Within the Fe-replete patch, viral abundance and production was on average 2- and 3-fold, respectively, higher than outside the patch. On average 40% of the bacteria contained viruses in a lytic stage inside the Fe-replete patch compared to 21% outside the patch. About 11–12% of the bacteria contained a viral genome inducible with mitomycin C in both inside and outside the patch. Randomly amplified polymorphic desoxyribonucleic acid polymerase chain reaction analysis suggested the development of a specific viral community in the patch. Although short-term stimulation of viral production was likely due to increased bacterial activity, the long-term stimulation was likely also influenced by an increased encounter rate between bacterial viruses and hosts. Viral lysis was responsible for most of the bacterioplankton mortality in the patch. Overall, most of the bacterial carbon production entered the detrital or dissolved organic matter pool via the viral shunt in the patch.

Iron is required for almost all life forms and participates in many biological processes such as respiration and desoxyribonucleic acid (DNA) synthesis (Andrews et al. 2003). Vast parts of the ocean are high-nutrient low-chlorophyll (HNLC) areas, now attributed to iron limitation. In several mesoscale in situ experiments it was shown that iron enrichment induced phytoplankton blooms leading to a draw-down of atmospheric CO_2 and transporting organic carbon out of the surface mixed layer (Boyd et al. 2007). Such experiments have also shown an enhancement of bacterial biomass and production in the Pacific (Cochlan 2001) and Southern Ocean (Hall and Safi 2001; Oliver et al. 2004). However, it is still unclear, whether bacteria in HNLC areas are iron- (Pakulski et al. 1996; Tortell et al. 1996) or carbon- and nitrogen-limited (Church et al. 2000; Kirchman et al. 2000). A certain level of co-limitation of Fe and organic carbon and nitrogen has also been observed (Church et al. 2000). Heterotrophic bacteria are responsible for 20–45% of biological iron uptake, compete directly with phytoplankton for iron (Tortell et al. 1996) and may thus be partially responsible for HNLC conditions.

Viruses infecting bacteria can play different roles in microbial food webs (Wommack and Colwell 2000). Lytic viruses infect cells, replicate and then destroy cells by lysis, setting free viral progeny and cellular lysis products. It was estimated that between 6% and 26% of photosynthetically fixed carbon will ultimately be shunted into the detrital and dissolved organic carbon pool by viral lysis of cells at all trophic levels (Wilhelm and Suttle 1999). This carbon can be used by bacteria and is, therefore, largely diverted from higher trophic levels, resulting in an overall stimulation of bacterial production and respiration (Fuhrman 1999). Thus, viruses can be seen as catalysts of carbon and nutrient cycling (Suttle 2005).

Temperate viruses remain within the cell in a dormant stage and replicate along with the hosts, until the lytic cycle is induced. It has been shown that solar radiation and hydrogen peroxide can induce the lytic cycle in marine bacterial communities (Jiang and Paul 1996; Weinbauer and Suttle 1999). Also, it was suggested that enhanced growth causes temperate viruses to enter the lytic cycle (Wilson and Mann 1997). The significance and nature of inducing agents in situ remain largely unknown. The association between temperate viruses and hosts can increase the fitness of the host by conferring morphologic or metabolic traits encoded in the viral genome and, thus, influence bacterial diversity and activity. To the best of our knowledge, nothing is known on the role of iron for marine lysogens or on responses of lysogenic bacterioplankton in iron-induced phytoplankton blooms.

The role of iron for viral dynamics is poorly studied. Poorvin et al. (2004) found that viral lysis regenerates iron, which can sustain a significant fraction of primary productivity, and Daughney et al. (2005) have shown that viruses might serve as nuclei for iron adsorption and precipitation. Mioni et al. (2005) demonstrated that

* Corresponding author: wein@obs-vlfr.fr

organically complexed iron in viral lysis products is highly bioavailable and Strzepek et al. (2005) report on highly variable virus-mediated iron regeneration rates during the FeCycle mesoscale experiment. During the EisenEx experiment, a phytoplankton bloom was induced upon iron addition and its development was followed for 3 weeks (Gervais et al. 2002). Bacterial biomass formation and enzymatic activity was enhanced as well and a short-term stimulation of bacterial activity could be observed (Arrieta et al. 2004). An enhanced bacterioplankton production and biomass could also result in a stimulation of viral production, either by enhanced infection or by a faster turnover of the microbial food web. Finally, an enhanced bacterial growth could also induce the lytic cycle in lysogenic bacterioplankton and thus, increase viral abundance without new infection. Here we report that viral production and infection of bacterioplankton were enhanced during the iron induced phytoplankton bloom of the EisenEx experiment, suggesting an important role of viral lysis for carbon and nutrient cycling.

Methods

Iron enrichment and sampling—The experiment was performed in the Atlantic sector of the Southern Ocean (21°E, 48°S) in austral spring (06–29 Nov 2000) during the cruise ANT XVIII/2 of RV *Polarstern*. For details consult Gervais et al. (2002). Briefly, a mesoscale eddy originating from the Polar Front was identified, fertilized with acidified iron sulfate solution and marked with the tracer SF_6. In addition, drifting buoys were placed into the fertilized water mass. Iron enrichment was repeated twice with intervals of 8 d and sampling was performed inside and outside the iron-enriched water mass. Samples were collected with a rosette sampler (Sea-Bird SBE 32) equipped with 24, 12-liter Niskin bottles, conductivity–temperature–depth probes (Sea-Bird Electronics SBE 911plus), and a Haardt fluorometer. For viral abundance, six samples were collected at each station between 10 m and 150 m depth. At selected stations, a large-volume water sample (150–200 liters) was collected from 20 m to 30 m depth for assessing viral production and infection of bacterioplankton.

Enumeration of viruses and bacteria; burst size—Samples for counting viruses and bacteria were preserved briefly (~30 min) in formaldehyde (2% final concentration) at 4°C. Samples of 1.5 mL were filtered onto 0.02-μm pore-size Anodisc filters (Whatman), stained with SYBR Green I (10,000× in dimethyl sulfide; Molecular Probes, Chemical No. S-7567; concentration of staining solution, 2.5×10^{-3} of stock), mounted in an anti-fade solution (glycerol, phosphate buffered saline, p-phenylenediamine), stored at −20°C and enumerated by epifluorescence microscopy as described by Noble and Fuhrman (1998). Data on bacterial abundance are reported in Arrieta et al. (2004).

To assess in situ burst size (i.e., the number of viruses released upon cell lysis), 1 mL of the bacterial concentrates (*see* below) from three stations inside and three stations outside the patch was preserved in glutaraldehyde (0.5% final concentration), kept briefly at 4°C and then stored at −80°C until analysis. Upon thawing, bacteria were collected by centrifugation onto formvar-coated transmission electron microscope (TEM) grids (copper, 400 mesh size) and stained with uranyl acetate (Weinbauer and Suttle 1999). The minimum burst size (BS) was estimated as average from ≥20 visibly infected cells. This number is a conservative estimate because viruses could still be assembled in the cells; therefore, a conversion was used to calculate maximum burst size (max. burst size = 1.41 min. BS + 0.87; Parada et al. 2006).

Bacterial production—Bacterial production rates in the viral production assays (*see* below) were estimated from the rate of [3H]-thymidine (Arrieta et al. 2004). A conversion factor of 1.1×10^{18} cells produced per mol thymidine was applied to convert thymidine incorporation to cell production (Fuhrman and Azam 1982). In situ data on thymidine and leucine incorporation reported below are from Arrieta et al. (2004).

Viral production and infection of bacterioplankton—Viral production, the fraction of infected cells (FIC) and the fraction of lysogenic cells (FLC) were estimated using a dilution technique (Wilhelm et al. 2002) with the modification described elsewhere (virus-reduction approach [VRA]; Weinbauer et al. 2002). Large water samples (150–200 liters) were filtered through 0.8-μm pore-size polycarbonate filters (142-mm diameter; Millipore) and bacteria were concentrated using a Pellicon (Millipore) tangential flow filtration system equipped with an 0.2-μm-filter cartridge (Durapore, Millipore) as described in (Arrieta et al. 2004). The first 20 liters of the 0.2-μm filtrate were processed with a 30 kDa cutoff polysulfone cartridge (Amicon S1) to produce virus-free water. Aliquots of the bacterial concentrate were added to virus-free water at roughly in situ abundance assuming that half of the bacteria were lost during the prefiltration and ultrafiltration step. This procedure reduces contact rates between viruses and hosts and, thus, new infection. Incubations were performed in the dark at in situ temperature (2.0–4.2°C) in duplicate 50-mL sterile conical tubes, which were acid-cleaned between experiments. Samples were typically taken at T0h, T4h, T8h, T12h, T18h and T24h.

Viral production (VP) was calculated as

$$VP = \frac{V_2 - V_1}{t_2 - t_1} \quad (1)$$

where V_1 and V_2 are viral abundances at t_1 and t_2 incubation times. Note that individual incubations were treated separately and values at the start of incubations were not always used for calculations. In contrast, the lower viral abundance serves as starting point for calculation (e.g., when viral abundance decreased after the start of the experiment). Thus, V_1 and V_2 are the minimum and maximum of viral abundance in the incubation. Dividing the number of produced viruses by the burst size yields the number of lysed cells and, thus, gives an estimation of FIC (Weinbauer et al. 2002). FIC

was calculated (as percentage) by

$$FIC = 100\frac{V_2 - V_1}{BS \times B} \quad (2)$$

where BS is the burst size and B is bacterial abundance at the start of the experiment. This treatment also served as control in the lysogeny bioassays. To induce lysogenic viruses, samples were treated with mitomycin C (Sigma Chemicals; final concentration, 1 μg mL^{-1}; Weinbauer et al. 2002). The difference in virus abundance between this treatment and the control is the number of induced viruses, which is divided by the burst size to estimate the number of induced cells and, thus, FLC. FLC was calculated as

$$FLC = 100\frac{VMC - VC}{BS \times B} \quad (3)$$

where VMC and VC is the maximum difference in viral abundance at corresponding time points in mitomycin C and control treatments, respectively.

Contact rates—The rate of contact (R) between viruses and bacteria was calculated using the following equations (Murray and Jackson 1992):

$$R = Sh \times 2w \times D_v \times V \times P \quad (4)$$

where Sh is the Sherwood number (1.06 for a bacterial community with 10% motile cells; Wilhelm et al. 1998), w is the equivalent spherical cell diameter (0.5 μm), V and P are the abundances of viruses and bacteria, respectively, and D_v is the diffusivity of viruses.

$$D_v = \frac{k \times T}{3 \times \pi \times \mu \times d_v} \quad (5)$$

where k is the Boltzmann constant (1.38 × 10–23 J Kelvin^{-1}), T is the in situ temperature (°Kelvin), μ is the viscosity of water (in Pascal s^{-1}) and d_v is the diameter of the viral capsid (60 nm). The contact rate was corrected for the bacterial abundance to estimate the number of contacts per cell on a daily basis.

Viral community fingerprint—Viral communities from 150 liters to 200 liters of 0.2 μm filtered water were concentrated to 200–300 mL using a 30-kDa cutoff cartridge (*see* above) and stored frozen at −80°C. Viruses were further concentrated to ~200 μL by centrifugation through 30-kD filters (Amicon Ultra-15; Millipore). Randomly amplified polymorphic DNA (RAPD) polymerase chain reaction (PCR) analysis was performed as described in Winget and Wommack (2008). Briefly, 2–50 ng of virioplankton DNA served as the template DNA in each reaction. For amplification, the decamer primer OPA-13 (5′-CAG CAC CCA C-3′) was used, acting as both, forward and reverse primer. PCR conditions are found in Winget and Wommack (2008). All RAPD-PCR products were separated by gel electrophoresis on 2.5% agarose gels in 1 TAE buffer at 9 V cm^{-1}, visualized by ethidium bromide (1 mg mL^{-1}) staining, and imaged in a gel imager (Intas). Similarity of resulting banding patterns was assessed by a group-averaged cluster analysis based on a Bray–Curtis similarity matrix and an analysis of similarity (ANOSIM). Uncertainty in the hierarchical cluster analysis of viral communities was calculated by multi-scale bootstrap resampling using the R package "pvclust" (http://cran.r-project.org/). Nonmetric Multidimensional Scaling (NMDS) was computed using function "metaMDS" of R package "vegan" with Bray–Curtis similarities.

Statistical analysis—In order to detect relationships between viral and bacterial parameters, a Pearson correlation matrix was calculated. Data were arcsine (for FIC and FLC after converting the percentage to fractions), square-root or log-transformed (all others). Parameters were also tested against time since iron addition. Differences of parameters inside and outside the Fe patch were tested for significance using a Mann–Whitney *U*-test. Significance level of $p < 0.05$ was assumed for statistical analysis.

Results

Description of study site and experimental approach—Sampling started on 07 November 2000, the day before the Fe enrichment started, and lasted for 22 d. Day 0 denotes the sampling directly after enrichment. Water temperature was <5°C and increased during the experiment by 0.7–1.5°C depending on the strata sampled. Chlorophyll *a* (Chl *a*) concentrations increased almost linearly after 4 d of the iron addition to values ~4-fold higher than at the start of the experiment (Gervais et al. 2002) and bacterial abundance increased during the first 12 d and remained then 2-fold higher inside compared to outside the patch (Arrieta et al. 2004). The Fe-fertilized patch, as identified by SF_6 concentrations, was initially confined to the top 40 m of the water column but extended in the third week to 80 m, probably due to mixing caused by storms (days 5–8 and 12–15).

Viral abundance and burst size—Generally, viral abundance increased inside the Fe-fertilized patch during the course of the experiment with elevated viral abundance down to 100-m depth towards the end of the experiment (Fig. 1). Viral abundance, averaged over the first 40 m, ranged from 2.3 × 106 mL^{-1} to 7.0 × 106 mL^{-1} inside and from 1.4 × 106 mL^{-1} to 2.5 × 106 mL^{-1} outside the patch. Although viral abundance increased inside the patch, despite some fluctuations, it remained comparatively constant outside the patch. Viral abundance integrated over time was 2.1 times higher in the patch than outside (Table 1). The depth-integrated values of viral abundance increased significantly with time within the Fe-enriched patch ($y = 27.66 + 1.49x$, $r^2 = 0.56$, $p < 0.01$). A similar regression ($y = 26.95 + 1.26x$, $r^2 = 0.52$, $p < 0.01$) was found when only viral abundances were used from the depth of the VRA incubations. The virus : bacteria ratio averaged 17 inside the patch and 12 outside the patch. Maximum BS ranged from 29 to 49 (average = 38) at six stations with no significant differences between inside (day 1, 9, and 22 after iron addition) and outside the patch (day 0, 8, and 19). Thus, the average BS value of 38 was used for calculations.

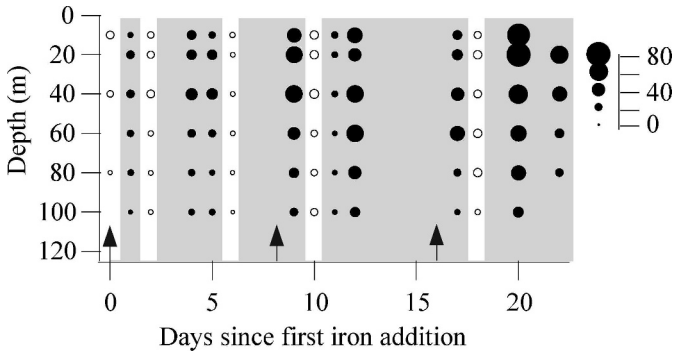

Fig. 1. Viral abundance along depth profiles during Fe enrichment. Symbols indicate inside (full circles, gray background) and outside (open circles, white background) of the Fe-enriched patch. The arrows at the bottom indicate the dates of Fe release. Units for viral abundance are given in 105 mL^{-1}.

Recovery efficiency of the viral production assays—Viral abundance in the viral production assays was reduced by ~80% of in situ abundances. Bacterial abundance in the virus reduction approach was 20–30% higher than in situ (Table 2). This suggests that the recovery efficiency of cells was ~70–80%, because we assumed a loss rate of 50% and adjusted volumes accordingly.

Viral production and bacterial mortality—Data on viral production and infection of bacterioplankton were obtained from samples collected in the Chl *a* maximum layer of the center of the Fe-fertilized patch. Viral production was corrected for the changes in bacterial abundance in the viral production assays (Fig. 2). Inside the patch, viral production was significantly higher (Mann–Whitney *U*-test, $p < 0.01$), averaging 1.90×10^6 mL^{-1} d^{-1} (range = $0.86 \times 10^6 - 3.63 \times 10^6$ mL^{-1} d^{-1}) than outside the patch (mean = 0.56×10^6 mL^{-1} d^{-1}, range = $0.33 \times 10^6 - 0.80 \times 10^6$ mL^{-1} d^{-1}; Fig. 2). For comparison, net viral production estimated from the increase in the viral abundance was 1.44×10^6 mL^{-1} d^{-1}. Viral production was more than three times higher 1 d after than directly before the Fe addition (Fig. 2). Viral production continued to increase until day 8 and dropped to values close to outside conditions afterwards. At the end of the survey, a second maximum occurred, which was slightly higher than the maximum at day 8. Viral production was 8–9-fold higher at the two maxima compared to the start of the experiment. On average, viral production was four times higher inside than outside the iron-fertilized patch (Table 1). Viral turnover averaged 0.52 d^{-1} (range = 0.15–1.05 d^{-1}) inside the patch and 0.27 d^{-1} (0.17–0.33 d^{-1}) outside the patch (Table 1). Lowest and highest viral turnover occurred at the same time as viral production; viral turnover and production were significantly correlated.

In situ bacterial production correlated with that in the VRA ($r^2 = 0.63$, $p < 0.0005$, $n = 12$) but was on average two times higher in the VRA than in situ. Virus-mediated mortality (VMM) of bacterioplankton was calculated in two ways (Table 2); first, using in situ bacterial production and in situ viral production (i.e., viral production in the VRA corrected for the changes in bacterial abundance during sample preparation; Fig. 2) and second, using bacterial and viral production data from the VRA incubation (given in Table 2). Outside the patch, VMM averaged 69% (range = 31–131%) using in situ production data and 39% (range = 14–70%) using production data from the VRA. Within the patch, estimates were 182% (range = 67–565%) for in situ production and 104% (range = 41–172%) for VRA. On average, estimates of VMM were approximately two times higher using in situ production compared to production in the VRA.

Viral infection of bacterioplankton and viral contact rates—The FIC ranged from 20% to 88% inside the patch, whereas it varied only little outside the patch ranging from 16% to 25% (Fig. 3a). On average, FIC was significantly (~2×) higher inside the patch (Mann–Whitney *U*-test, $p < 0.05$). Maximums of FIC coincided with peaks in viral production (i.e., at day 8 and 22). Maximum FIC was 3.1- and 5.4-fold higher inside the patch than at the start of the experiment (Fig. 4a). The FLC was similar inside (range = 5–17%; average = 11%) and outside the patch (range = 5–16%; average = 13%; Fig. 3b). Inside the patch, FLC values decreased slightly from day 0 to day 8, and from day 20 to 22, but increased in between to levels roughly similar to that of day 0. No significant differences were found in

Table 1. Average values and ranges (in brackets) of viral parameters inside and outside the Fe-fertilized patch. The average ratio of parameters between inside and outside the patch is also shown. Parameters significantly different (Mann–Whitney *U*-test, $p < 0.05$) between inside and outside the Fe-fertilized patch are in bold.

Parameter*	Inside			Outside			Average ratio
	Mean	Range	SE	Mean	Range	SE	
FIC (%)	40	20–88	10	21	26–24	2	**1.9**
FLC (%)	11	5–17	2	12	5–16	2	0.9
Viral production (10^6 mL^{-1} d^{-1})	1.90	0.86–3.63	0.48	0.56	0.33–0.80	0.09	**3.3**
Burst size	40	34–49	4	36	29–42	4	1.1
Viral abundance (10^6 mL^{-1})	4.3	2.3–7.0	5.5	2.1	1.4–2.5	2.0	**2.1**
Viral contacts per cell (d^{-1})	15	8–25	1	7	5–8	2	**2.1**
Viral turnover (d^{-1})	0.52	0.15–1.05	0.12	0.27	0.17–0.33	0.03	**1.9**

* FIC = fraction of infected cells; FLC = fraction of lysogenic cells. Note that burst size data represent only three samples from each, inside and outside the patch. Viral abundance was averaged over the first 40 m. For viral turnover, viral abundance from the water samples collected for the viral-reduction approach (VRA) incubations was used.

Table 2. Evaluating the virus reduction approach (VRA) for estimating viral production and virus-induced losses of bacterial production inside and outside the Fe-fertilized patch. Note that viral production data in Fig. 2 were corrected for changes in bacterial abundance.

Day	$BP_{in\ situ}$ (10^4 mL^{-1} d^{-1})*	BP_{VRA} (10^4 mL^{-1} d^{-1})*	BA_{VRA} : $BA_{in\ situ}$*	VP_{VRA} (10^6 mL^{-1} d^{-1})*	% $BP_{in\ situ}$ lysed*	%BP_{VRA} lysed*
Inside						
Day 1	3.4	5.6	1.22	1.73	110	80
Day 4	3.8	7.1	1.35	3.19	164	118
Day 8	1.4	6.5	1.42	4.25	565	172
Day 9	1.4	4.9	1.33	1.15	163	62
Day 13	3.8	7.2	1.28	1.97	107	72
Day 17	5.4	9.4	1.05	1.44	67	41
Day 20	2.1	2.6	1.44	1.49	130	149
Day 22	6.1	8.6	1.26	4.58	157	139
Average	3.4	6.5	1.29	2.48	182	104
Outside						
Day 0	2.4	3.8	1.01	0.53	58	37
Day 2	2.1	4.2	1.29	0.43	42	26
Day 6	3.8	8.9	1.07	0.48	31	14
Day 10	2.5	4.1	0.99	0.79	84	50
Day 18	1.4	3.2	1.23	0.86	131	70
Average	2.4	4.9	1.19	0.62	69	39

* BP = bacterial production; BA = bacterial abundance; VP = viral production. In situ bacterial abundance and production data are from Arrieta et al. (2004).

FLC inside and outside the Fe-fertilized patch (Mann–Whitney *U*-test, $p > 0.2$). Viral contact rates were significantly higher inside (average = 15 cell^{-1} d^{-1}; range = 8–25 cell^{-1} d^{-1}) than outside the patch (average = 7 cell^{-1} d^{-1}; range, 4–8 cell^{-1} d^{-1}; Mann–Whitney *U*-test, $p < 0.05$).

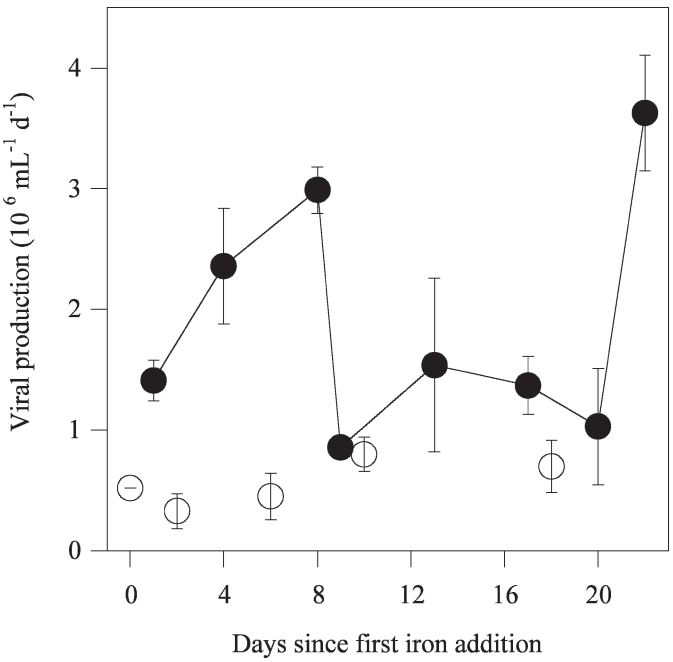

Fig. 2. Viral production during Fe enrichment. Bars indicate the range of duplicate incubations. Data were corrected for the differences in bacterial abundance in the VRA compared to in situ. Symbols indicate inside (full circles) or outside (open circles) of the Fe-enriched patch.

Correlation analysis of data inside and out of the patch—When testing viral parameters against time elapsed in the mesoscale experiment, viral abundance in the patch was the only parameter that showed a significant correlation. Data transformation did not increase correlation coefficients (data not shown). It has been shown before that bacterial production and enzymatic activity did not change linearly with time, whereas there was a slightly positive correlation for bacterial abundance (Arrieta et al. 2004).

The results of the correlation analysis of viral and bacterial parameters outside and inside the patch are shown in Table 3 for parameters exhibiting a significant relationship with viral parameters. Outside the patch, FIC increased with bacterial abundance and viral abundance increased with thymidine incorporation. Inside the patch, FIC increased with viral production and leucine incorporation, whereas FLC was negatively related to thymidine incorporation. A strong correlation was found between viral and bacterial abundance.

Viral community composition—The viral community fingerprinting by RAPD-PCR revealed 6–15 distinguishable bands for the individual samples (i.e., viral communities), from inside and outside the patch. The lowest number of bands was found outside and the highest inside the patch (Fig. 4a). Viral community composition was similar at several time points; however, band patterns did also vary strongly both inside and outside the patch. Based on ANOSIM, no significant differences between inside and outside the patch were found ($R = 0.1667$, $p = 0.099$). However, when the first sample taken after Fe addition was

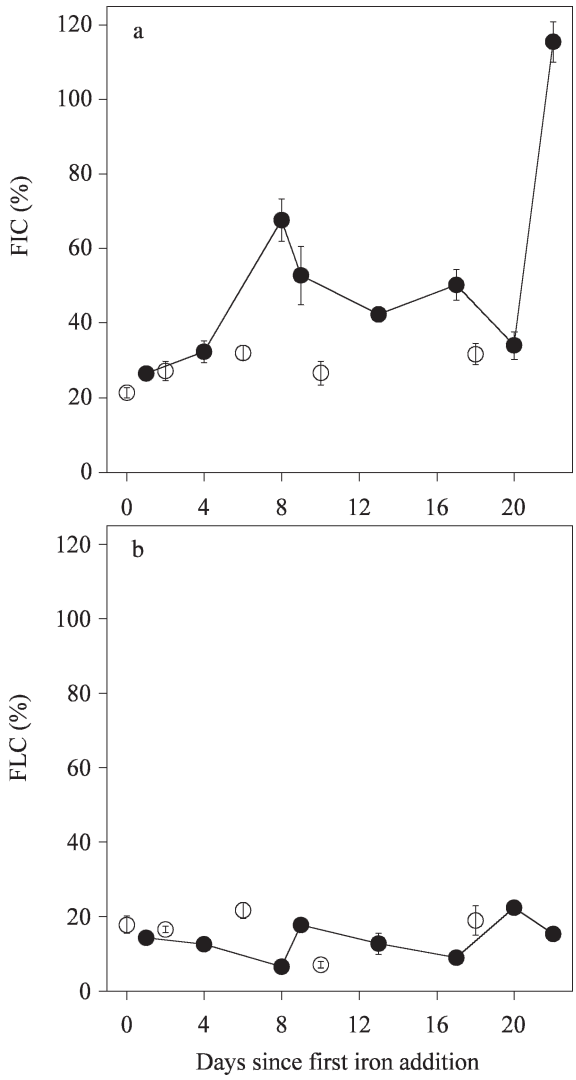

Fig. 3. Viral infection of bacterioplankton during Fe enrichment. (a) Lytic-stage and (b) lysogenic infection. Bars indicate the range of duplicate incubations. Symbols indicate inside (full circles) or outside (open circles) of the Fe-enriched patch. FIC = fraction of lytically infected cells; FLC = fraction of lysogenic cells.

removed, differences between inside and outside the patch were significant ($R = 0.358$, $p = 0.023$). Using NMDS, one can define a path of change in the viral communities. Fig. 4b shows that the community inside the patch changed continuously and followed a different path than the outside community (at least starting from day 4).

Discussion

Evaluation of approaches used to assess VMM—Inside the Fe-fertilized patch, VMM estimates based on in situ bacterial production were in almost all samples higher than 100% of bacterial production. In steady state, a VMM higher than 100% means a decrease of abundance; however, we found an increase of bacterial abundance in the patch (Arrieta et al. 2004). In contrast, using bacterial production in the VRA, VMM was on average ~100% and hence, appears to be more realistic than the estimates based on in situ bacterioplankton production. It is noteworthy that bacterial production in situ and in the VRA was related, although bacterial production in the VRA was higher probably due to the release of organic matter from cells during filtration. Nevertheless, VMM estimates using bacterial production in the VRA were sometimes too high to be sustained. Similar conclusions have been reported previously for other environments as well (Helton et al. 2005; Winget et al. 2005).

Several potential explanations are discussed below to explain this apparent discrepancy. Manipulations during the VRA approach could stimulate viral production (e.g., by stimulating burst size). However, some data suggest that the VRA does not influence the burst size, because different dilutions, which changed bacterial growth rates, did not affect FIC values (Weinbauer et al. 2002). This is further supported by the finding that the burst size of bacterioplankton collected in situ was essentially the same as in the VRA (Weinbauer and Suttle 1999). Nevertheless it is known that, in situ, the burst size can increase with bacterial production (Parada et al. 2006). Therefore, we cannot exclude the possibility that the strong enhancement of bacterial production in the VRA increased burst size and, thus, viral production. Bacterial production was stimulated in pulses following the iron additions inside the fertilized patch but otherwise presented similar average values inside and outside the patch (Arrieta et al. 2004). This could be one of the reasons why the burst size was similar inside and outside the patch. Although we used maximum burst size estimates, we cannot fully exclude the possibility of a TEM-based underestimation of the burst size, possibly due to failing to distinguish or identify all viral particles using the whole cell approach. Such an underestimation of the burst size would result in an overestimation of virus-mediated mortality. The average value of 38 is similar to the average maximum burst size of 42 for the Southern Ocean (Strzepek et al. 2005) calculated by using the correction of Parada et al. (2006). In addition, it might not be the burst size that is changed but the rate at which viruses are produced. This would result in an overestimation of VMM estimated based on viral production rates. Such a mechanisms might explain why mortality estimates based on FIC are often more realistic than estimates based on viral production in a single VRA (Winter et al. 2004*a*; Winter et al. 2005). Also, the reduced contact rates in the incubations, could result in less infection and lysis and thus, in increased bacterial production. Finally, it is well-know that relating the incorporation of a radiolabeled substrate to cell production is problematic, even if habitat-specific conversion factors are determined (Robarts 1998), which, was not done in the present study. Thus, an underestimation of bacterial cell production by the thymidine incorporation method could have contributed to an overestimation of mortality.

It has been shown that the VRA results in ecologically meaningful trends of VMM such as changes along fronts (Wilhelm et al. 2002), trophic gradients (Helton et al. 2005; Winget et al. 2005) or diel (Winter et al. 2004*a*) and seasonal variations (Winter et al. 2005). Our study supports

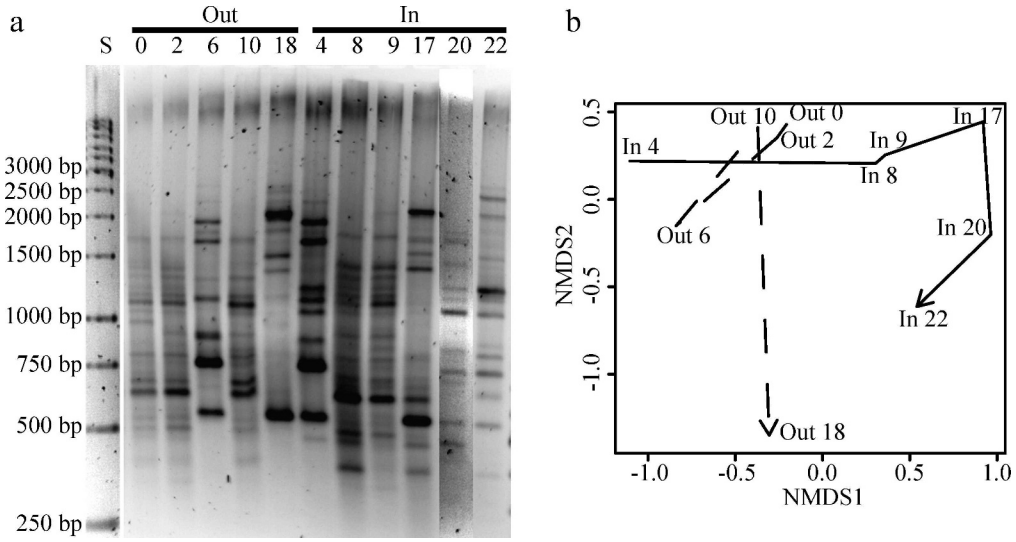

Fig. 4. Viral community composition during Fe enrichment. (a) RAPD-PCR gel and (b) Nonmetrical multidimensional scaling analysis. Numbers on top of the gel refer to days after iron enrichment. In = inside the patch; Out = outside the patch; S = DNA size marker in base pairs (bp).

these findings. For example, VRA showed that FIC was enhanced inside compared to outside the patch, whereas there was no difference for FLC. In addition, FIC was positively, while FLC was negatively related to bacterial production. Such a pattern was also detected in other systems (Weinbauer et al. 2003).

Table 3. Matrix of correlation coefficients of viral parameters* outside and inside the Fe-fertilized patch. For units *see* Table 1. Significant correlation coefficients ($p < 0.05$) are shown in bold. The coefficient for which values are significant differs between inside and outside the patch due to different number of samples. Only those parameters that significantly correlate with viral parameters are shown.

	FIC	FLC	VP	VA
Inside				
FIC	1			
FLC	−0.327	1		
VP	**0.656**	0.216	1	
VA	0.385	−0.354	−0.144	1
BP-Leu	**0.665**	−0.408	0.084	0.491
BP-Thy	0.550	**−0.623**	0.127	0.471
BA	0.506	−0.035	0.005	**0.907**
Outside				
FIC	1			
FLC	0.354	1		
VP	−0.585	0.371	1	
VA	−0.457	−0.653	0.050	1
BP-Leu	0.235	−0.252	−0.347	0.661
BP-Thy	0.238	−0.565	−0.422	**0.817**
BA	**0.928**	0.270	−0.539	−0.138

* FIC = frequency of infected cells; FLC = frequency of lysogenic cells; VP = viral production rates; VA = viral abundance; BP = bacterial production rates; Leu = leucine incorporation; Thy = thymidine incorporation; BA = bacterial abundance. Data on bacterial abundance and production are from Arrieta et al. (2004). All data are from the depth of the virus reduction approach (VRA) incubations.

Mesoscale iron enrichment experiments and viruses—The mesoscale iron-enrichment studies performed so far have shown a stimulation of primary and bacterial production and biomass (Boyd et al. 2007) compared to so-called out-stations. Out-stations can represent different water masses (consequently, data are usually not given as line charts) and thus, are not real controls (Arrieta et al. 2006). However, they serve as an indication of the "background" variability (Arrieta et al. 2006). In this sense, sampling different water masses is beneficial, because differences in the iron patch compared to outside the patch, as found in our study and in others of the EisenEx campaign (Arrieta et al. 2004; Gervais et al. 2002), are very likely due to the iron enrichment. FeCycle is the only other mesoscale iron-enrichment experiment, where viral parameters have been published. However, data were not compared to out-stations (Strzepek et al. 2005). Inside the patch, viral production in FeCycle from the Southern Ocean ranged from 0.04×10^6 mL^{-1} d^{-1} to 2.35×10^6 mL^{-1} d^{-1} (Strzepek et al. 2005), which is similar to our data from within the patch ($0.86–3.63 \times 10^6$ mL^{-1} d^{-1}) albeit more variable. Burst size averaged 42 after applying the correction of Parada et al. (2006), which is similar to the estimate of 38 for EisenEx. During a survey in the Southern Ocean, the development of a phytoplankton bloom, which was induced by iron release from the sediment, was monitored over the shelf of the Kerguelen Islands and this situation was compared to the surrounding HNLC area (Christaki et al. 2008). Viral production and infection of bacterioplankton were higher in the bloom than in the HNLC stations (M. G. Weinbauer unpubl.); thus, supporting our findings of higher VMM in the patch. Nevertheless, further studies in the sense of further replications have to be performed to confirm the observed increased viral production and infection in iron-stimulated phytoplankton blooms and its effect on an ecosystem level.

Table 4. Independent approaches to assess virus-mediated mortality (VMM) of bacterioplankton inside and outside the Fe-fertilized patch. Data calculation is specified in the text. For viral-abundance–based data, the first number is from integrated values and the second from values when the VRA was performed. Release rates were calculated from VMM and from rates and cell quotas given in Arrieta et al. (2004) and Strzepek et al. (2005); for details *see* text.

	VMM (%) based on			Release based on VMM	
	Viral production	FIC	Increase of in situ viral abundance	pmol Fe L^{-1} d^{-1}	μmol C L^{-1} d^{-1}
Inside	104	95	128;102	0.67–0.90	0.085–0.115
Outside	40	31	Na*	0.15–0.20	0.020–0.026

* Na = not applicable.

Estimation of virus-mediated mortality of bacterioplankton—It is possible that other viruses than bacteriophages contributed to the increase in viral abundance during the Fe-enrichment, because not only bacteria (Arrieta et al. 2004) but also phytoplankton (Gervais et al. 2002) increased in biomass in the Fe-enriched patch. However, viruses infecting phytoplankton constitute only a minor fraction of the viral community (except for cyanoviruses, which might be occasionally abundant [Maranger and Bird 1995]). Cyanobacterial abundance was low at the study site (Gervais et al. 2002). Moreover, viral and bacterial abundance inside the patch were more strongly correlated (Table 3; $r = 0.907$) than viruses and Chl *a* ($r = 0.748$; calculated using data published in Gervais et al. [2002]). Thus, the majority of the viruses were likely viruses infecting the domain bacteria and the increase in viral abundance during the experiment was, therefore, mainly due to lysis of bacterial cells.

Using the increase of viral abundance over time, a burst size of 38 and the mean bacterial production inside the patch (Table 2), viruses should have lysed 127% (using integrated values) and 102% (using only values from the VRA) of the bacterial production (Table 4). Using viral production data, VMM was on average ~104% inside the patch (using bacterial production in the VRA). In addition, relating FIC to VMM by the model of Binder (Binder 1999), VMM was on average 95% inside the patch. For outside the patch, the values were 40% for viral-production–based estimates and 31% for FIC-based estimates. Thus, the data indicate that VMM was 2–3-fold higher inside than outside the patch. It is noteworthy that independent approaches or calculations provided similar average estimates (Table 4).

Additional support comes from the following calculation from within the patch using published data. From bacterial production data (Arrieta et al. 2004) we can calculate the bacterial abundance expected at the next time point. The difference of this value from the observed bacterial abundance (Arrieta et al. 2004) is an estimation of bacterial mortality. Assuming that all mortality is due to viral lysis and using the observed burst size of 38, the expected viral abundance can be calculated and compared to the observed viral abundance. Averaging the data over the study period, the observed viral abundance was 78% of the expected viral abundance as calculated using thymidine incorporation to determine bacterial production and 111% using leucine incorporation. The finding that observed values were ~100% of expected values supports our estimations from different approaches that viral lysis was by far the most important mortality factor for bacterioplankton within the patch.

Comparison of virus infection data with other offshore studies—Lytic-stage virus infection can be due to lytic viruses, temperate viruses directly entering the lytic cycle after infection or the induction of lysogenic cells. Low values of about 10% lytic-stage virus infection of bacterioplankton were reported for offshore surface waters of the Mediterranean Sea (Weinbauer et al. 2003) and even lower values in another study (Guixa-Boixereu et al. 1999). In the tropical Atlantic, FIC values of 5–12% were found in offshore surface waters (Winter et al. 2004*b*). We found that under Fe limitation (i.e., outside the patch), a significant fraction of the bacterioplankton (21%) contained viruses in the lytic stage. It has been argued that a high virus-induced mortality of bacterioplankton in Antarctic waters is due to low water temperature, which is unfavorable for protist grazers (Guixa-Boixereu et al. 2002). Indeed, a high viral effect on bacterioplankton (up to 36% of bacterial production) was found in the cold North Atlantic and Arctic waters (Middelboe et al. 2002; Steward et al. 1996).

FLC values of, on average, 12% have been reported for offshore surface waters in the Mediterranean Sea (Weinbauer et al. 2003) and values of 2–11% for offshore waters in the Gulf of Mexico (Weinbauer and Suttle 1999). Contrasting trends along coastal–offshore transects and higher FLC values have been found as well (Jiang and Paul 1996). On average, our FLC values of 5–17% are comparable with the few data available for offshore surface waters.

More than 30% of the bacteria outside the patch contained a functional (lytic or temperate) virus genome. This value is similar to those reported for offshore surface waters of the Mediterranean Sea (Weinbauer et al. 2003). This further stresses the significance of viral infection for bacteria-mediated processes in the ocean.

Virus infection and iron amendment—The rapid response of bacteria to iron enrichment in the Southern Ocean during EisenEx might indicate iron limitation, although elevated supply of freshly released organic carbon by phytoplankton in the Fe-fertilized patch as compared to outside the patch likely contributed to the observed bacterial response as well (Arrieta et al. 2004). A rapid increase bacterial production

4 h after Fe enrichment was shown for the subtropical Pacific (Mioni et al. 2007). FIC (day 4) and viral production (day 1 and 4) were stimulated shortly after iron addition (Figs. 3, 4). Bacterial production during EisenEx showed short pulses right after Fe addition as well (Arrieta et al. 2004). Viral community composition also changed rapidly after the three Fe additions. This suggests that bacterial activity enhanced viral production. Induction of lysogenic bacteria due to relieving iron stress from bacteria and/or increased bacterial growth rates could have caused this increased bacterial mortality inside the patch. However, because FLC was low and did not differ between inside and outside the patch, induction cannot explain the increase of FIC within the patch. Thus, lytic viruses or temperate viruses directly entering the lytic cycle after infection were mainly responsible for the stimulated viral production and VMM of bacterioplankton during iron enrichment.

An enhanced bacterial production may, on the one hand, allow for higher infection frequencies (e.g., due to a higher expression of receptors as docking sites for viruses) and, on the other hand, increase viral production rates even if the same percentage of cells is infected. It is known that some viruses use the iron uptake system as receptors for attachment to the cell (Lenski 1988). The finding that outer membrane receptor for siderophores (i.e., extracellular high-affinity iron-uptake ligands), are only expressed during Fe limitation has been interpreted as a strategy to reduce the targeting of the outer membrane receptors by viruses and confer temporal resistance (Andrews et al. 2003). Because FIC increased within the patch, such a possible protection mechanism could not prevent an increase of virus infection during the mesoscale Fe-addition experiment. However, bacterial production and cell-specific leucine and thymidine incorporation rates peaked briefly after each of the Fe amendments (Arrieta et al. 2004). Also, a significant induction of hydrolytic ectoenzymes was observed inside the Fe-fertilized patch (Arrieta et al. 2004), which should have been accompanied by enhanced synthesis of the corresponding uptake systems. These surface-associated hydrolases and uptake systems could serve as viral receptors, resulting in increasing infection rates. In addition, bacterial abundance increased inside the patch (Arrieta et al. 2004) and viral contacts per cell were twice as high inside as outside the patch (Table 2). Possibly, an increased bacterial activity and an enhanced contact rate acted synergistically during the experiment and resulted in an increase of virus infection and viral abundance inside compared to outside the Fe fertilized patch.

Multidimensional scaling analysis revealed that in the Fe-enriched patch a specific viral community developed. The finding of a rather stable bacterial (Arrieta et al. 2004) and a specific viral community could be explained by viral control of bacterial phylotypes, which would out-compete other members of the bacterial community. Such a keeping in check of consecutively changing bacterial winners for nutrient acquisition could result in strong changes of the viral community and keep bacterial composition relatively stable. This is compatible with the idea that the virus-susceptible phylotypes can be low in number but have a high potential growth rate (Bouvier and del Giorgio 2007). An alternative scenario is that the development of resistance in a phylotype reduces infection rates and abundance of a specific virus and allows the increase of other viruses. Thus, a succession of different viral types with an overlapping or identical host range and changing resistance patterns could also explain a relatively stable bacterial and a dynamic viral community. Such scenarios are based on assumptions such as that the viral community was mainly composed of bacteriophages (*see* above), RAPDs are a useful proxy for viral community composition (Winget and Wommack 2008) and terminal restriction fragment length polymorphisms patterns are a useful proxy for the bacterial community (Arrieta et al. 2004). Our data suggests that the higher infection of bacterioplankton inside the patch is caused by an interplay of phenotypic and genotypic effects.

Role of viral lysis for biogeochemical processes—Despite some uncertainty about the absolute values, our data suggest that viruses were an important mortality factor for bacterioplankton outside the patch and the major factor within the patch. Interestingly, during a study in the Southern Ocean around the Kerguelen Island plateau, bacterial mortality due to protistan grazing was high in the HNLC area, but negligible in the phytoplankton bloom (Christaki et al. 2008), whereas viral infection showed the opposite trend (M. G. Weinbauer unpubl.). These data suggest a switch from grazing to viral lysis as the main control mechanism of bacterial biomass and a change of the fate of bacterial carbon production due to iron addition.

Viral lysis of bacterioplankton results in a reduced carbon flow to higher trophic levels via grazing of bacteria by protists; this and the release of lysis products can fuel bacterial growth (Fuhrman 1999; Middelboe et al. 2003). We estimated that a significant fraction of the bacterial production within the patch (up to 100%; Table 4) should be diverted from being utilized by higher trophic levels, shunted into the detrital and dissolved organic matter pool (Wilhelm and Suttle 1999), and become available to (infected and noninfected) bacteria. Using the conversion factors and cell quotas from Strzepek et al. (2005), average thymidine incorporation data from Arrieta et al. (2004) and assuming VMM from Table 4, 0.085–0.115 μmol C L^{-1} d^{-1} would be released (Table 4). In addition, data suggest that viral lysis reduces the growth efficiency and increases respiration rates of bacterioplankton (Middelboe et al. 1996). This has also been shown for the Southern Ocean and could increase remineralization rates (Bonilla-Findji et al. 2008).

Viral lysis has several potential consequences for iron and carbon cycling. Enhanced production of mainly colloidal organic iron as the result of viral lysis of bacteria during natural and anthropogenic Fe additions would retain reduced and bioavailable Fe in the euphotic zone. Using the conversion factors and cell quotas from Strzepek et al. (2005), average thymidine incorporation data from Arrieta et al. (2004) and assuming VMM from Table 4, 0.67–0.90 pmol Fe L^{-1} d^{-1} would be released. This is at the lower range of values (0.4–28 pmol Fe L^{-1} d^{-1}) reported before for viral lysis (Strzepek et al. 2005). Retaining iron could be significant during natural ephemeral Fe dust-fall events or when icebergs melt in HNLC

zones. With respect to the potential of relieving iron limitation as a mechanism stimulating carbon sequestration and export, an increased release of lysis products could result in a reduced carbon sequestration because viral lysis converts living particulate organic matter to nonliving dissolved and detrital organic matter, which is finally respired. However, the actual outcome of an increased viral lysis by Fe pulses will depend on whether the major consequence is an increased retention time and organic matter oxidation or an increased Fe regeneration.

Acknowledgments

We are grateful to V. Smetacek for the invitation to the EisenEx cruise and providing the opportunity to perform this work. The expertise of V. Strass (physical oceanography), A. Watson (SF_6 measurements), H. de Baar (Fe measurements), and their coworkers has made this work possible. Also, we thank the officers and the crew of the RV *Polarstern* for their support. S. Schmidt is acknowledged for support in statistical analysis. Two anonymous referees provided very valuable comments. Financial support was provided by the Earth and Life Sciences of the Dutch Research Council (ALW-NWO), the Royal Netherlands Institute for Sea Research (NIOZ), and the French Science Ministry (ANR-AQUAPHAGE). J. M. A. was supported by a predoctoral grant from the Basque Government.

References

Andrews, S. C., A. K. Robinson, and F. Rodriguez-Quinones. 2003. Bacterial iron homeostasis. FEMS Microbiol. Rev. **27:** 215–237.

Arrieta, J. M., M. G. Weinbauer, and G. J. Herndl. 2006. Response to: "Interpreting the results of oceanic mesoscale enrichment experiments: Caveats and lessons from limnology and coastal ecology" by M. S. Hale and R. B. Rivkin. Limnol. Oceanogr. **52:** 916–918.

———, M. G. Weinbauer, C. Lute, and G. J. Herndl. 2004. Response of bacterioplankton to iron addition in the Southern Ocean. Limnol. Oceanogr. **49:** 799–808.

Binder, B. 1999. Reconsidering the relationship between virally induced bacterial mortality and frequency of infected cells. Aquat. Microb. Ecol. **18:** 207–215.

Bonilla-Findji, O., A. Malits, D. Lefèvre, E. Rochelle-Newall, L. Lemée, M. G. Weinbauer, and J.-P. Gattuso. 2008. Viral effects on bacterial respiration, production and growth efficiency: Consistent trends in the Southern Ocean and the Mediterranean Sea. Deep-Sea Res. Part II **55:** 790–800.

Bouvier, T., and P. A. del Giorgio. 2007. Key role of selective viral-induced mortality in determining marine bacterial community composition. Environ. Microbiol. **9:** 287–297.

Boyd, P. W., and others. 2007. Mesoscale iron enrichment experiments 1993–2005: Synthesis and future directions. Science **315:** 612–617.

Christaki, U., I. Obernosterer, F. van Wambeke, M. Veldhuis, N. Garcia, and P. Catala. 2008. Microbial food wen structure in a naturally iron-fertilized area in the Southern Ocean (Kerguelen Plateau). Deep-Sea Res. Part II **55:** 706–719.

Church, M. J., D. A. Hutchins, and H. W. Ducklow. 2000. Limitation of bacterial growth by dissolved organic matter and iron in the Southern ocean. Appl. Environ. Microbiol. **66:** 455–466.

Cochlan, W. 2001. The heterotrophic bacterial response during a mesoscale iron enrichment experiment (IronEx II) in the eastern equatorial Pacific Ocean. Limnol. Oceanogr. **46:** 428–435.

Daughney, C., X. Chatellier, A. Chan, P. Kenward, D. Fortin, C. A. Suttle, and D. A. Fowle. 2005. Adsorption and precipitation of iron from seawater on a marine bacteriophage (PWH3a-P1). Mar. Chem. **91:** 101–115.

Fuhrman, J. A. 1999. Marine viruses and their biogeochemical and ecological effects. Nature **399:** 541–548.

———, and F. Azam. 1982. Thymidine incorporation as a measure of heterotrophic bacterioplankton production in marine surface waters: Evaluation and field results. Mar. Biol. **66:** 109–120.

Gervais, F., U. Riebesell, and M. Y. Gorbunov. 2002. Changes in primary productivity and chlorophyll a in response to iron fertilization in the Southern polar frontal zone. Limnol. Oceanogr. **47:** 1324–1335.

Guixa-Boixereu, N., D. Vaqué, J. Gasol, and C. Pedros-Alio. 1999. Distribution of viruses and their potential effect on bacterioplankton in an oligotrophic marine system. Aquat. Microb. Ecol. **19:** 205–213.

———, ———, ———, J. Sanchez-Camara, and C. Pedros-Alio. 2002. Viral distribution and activity in Antarctic waters. Deep-Sea Res. Part II **49:** 827–845.

Hall, J., and K. Safi. 2001. The impact of in situ Fe fertilization on the microbial food web in the Southern Ocean. Deep-Sea Res. Part II **48:** 2591–2613.

Helton, R., M. Cottrell, D. Kirchman, and K. E. Wommack. 2005. Evaluation of incubation-based methods for estimating virioplankton production in estuaries. Aquat. Microb. Ecol. **41:** 209–219.

Jiang, S. C., and J. H. Paul. 1996. Occurrence of lysogenic bacteria in marine microbial communities as determined by prophage induction. Mar. Ecol. Prog. Ser. **142:** 27–38.

Kirchman, D., B. Meon, M. Cottrell, and D. Hutchins. 2000. Carbon versus iron limitation of bacterial growth in the California upwelling regime. Limnol. Oceanogr. **45:** 1681–1688.

Lenski, R. E. 1988. Dynamics of interactions between bacteria and virulent bacteriophage. Adv. Microb. Ecol. **10:** 1–44.

Maranger, R., and D. F. Bird. 1995. Viral abundance in aquatic systems: A comparison between marine and fresh waters. Mar. Ecol. Prog. Ser. **121:** 217–226.

Middelboe, M., N. O. G. Jørgensen, and N. Kroer. 1996. Effects of viruses on nutrient turnover and growth efficiency of noninfected marine bacterioplankton. Appl. Environ. Microbiol. **62:** 1991–1997.

———, T. Nielsen, and P. Bjørnsen. 2002. Viral and bacterial production in the North Water: In situ measurements, batch culture experiments and characterization and distribution of a virus-host system. Deep-Sea Res. Part II **49:** 5063–5079.

———, L. Riemann, C. Steward, W. Hannsen, and O. Nybroe. 2003. Virus-induced transfer of organic carbon released between marine bacteria in a model community. Aquat. Microb. Ecol. **33:** 1–10.

Mioni, C. E., J. D. Pakulski, L. Poorvin, A. Baldwin, M. R. Twiss, W. H. Jeffrey, and S. W. Wilhelm. 2007. Variability in the in situ bioavailability of Fe to bacterioplankton communities in the eastern subtropical Pacific Ocean. Aquat. Microb. Ecol. **46:** 239–251.

———, L. Poorvin, and S. W. Wilhelm. 2005. Virus and siderophore-mediated transfer of available Fe between heterotrophic bacteria: Characterization using an Fe-specific bioreporter. Aquat. Microb. Ecol. **41:** 233–245.

Murray, A. G., and G. A. Jackson. 1992. Viral dynamics: A model of the effects of size, shape, motion and abundance of single-celled planktonic organisms and other particles. Mar. Ecol. Prog. Ser. **89:** 103–116.

Noble, R. T., and J. A. Fuhrman. 1998. Use of SYBR Green I for rapid epifluorescence counts of marine viruses and bacteria. Aquat. Microb. Ecol. **14:** 113–118.

Oliver, J. L., R. T. Barber, W. O. Smith, and H. W. Ducklow. 2004. The heterotrophic bacterial response during the Southern Ocean Iron Experiment (SOFeX). Limnol. Oceanogr. **49:** 2129–2140.

Pakulski, J., and others. 1996. Iron stimulation of Antarctic bacteria. Nature **383:** 133–134.

Parada, V., G. J. Herndl, and M. G. Weinbauer. 2006. Viral burst size of heterotrophic prokaryotes in aquatic systems. J. Mar. Biol. Assoc. UK **86:** 613–621.

Poorvin, L., J. Rinto-Kantp, D. A. Hutchins, and S. Wilhelm. 2004. Viral release of iron and its bioavailability to marine plankton. Limnol. Oceanogr. **49:** 1734–1741.

Robarts, R. 1998. Incorporation of radioactive precursors into macromolecules as measures of bacterial growth: Problems and pitfalls, p. 472–486. *In* K. Cooksey [ed.], Molecular approaches to the study of the ocean. Chapman and Hall.

Steward, F. G., D. C. Smith, and F. Azam. 1996. Abundance and production of bacteria and viruses in the Bering and Chukchi Sea. Mar. Ecol. Prog. Ser. **131:** 287–300.

Strzepek, R. F., M. T. Maldonado, J. L. Higgins, J. Hall, K. Safi, S. W. Wilhelm, and P. W. Boyd. 2005. Spinning the "Ferrous Wheel": The importance of the microbial community in an iron budget during the FeCycle experiment. Glob. Biogeochem. Cycles **19:** GB4S26, doi:10.1029/2005GB002490.

Suttle, C. A. 2005. Viruses in the sea. Nature **437:** 356–361.

Tortell, P. D., M. T. Maldonando, and N. M. Price. 1996. The role of heterotrophic bacteria in iron-limited ocean systems. Nature **383:** 330–332.

Weinbauer, M., I. Brettar, and M. Höfle. 2003. Lysogeny and virus-induced mortality of bacterioplankton in surface, deep, and anoxic waters. Limnol. Oceanogr. **48:** 1457–1465.

———, C. Winter, and M. Höfle. 2002. Reconsidering transmission electron microscopy based estimates of viral infection of bacterioplankton using conversion factors derived from natural communities. Aquat. Microb. Ecol. **27:** 103–110.

Weinbauer, M. G., and C. A. Suttle. 1999. Lysogeny and prophage induction in coastal and offshore bacterial communities. Aquat. Microb. Ecol. **18:** 217–225.

Wilhelm, S. W., S. Brigden, and C. Suttle. 2002. A dilution technique for the direct measurement of viral production: A comparison in stratified and tidally mixed coastal waters. Microb. Ecol. **43:** 168–173.

———, and C. A. Suttle. 1999. Viruses and nutrient cycles in the Sea. Bioscience **49:** 781–788.

———, M. G. Weinbauer, C. A. Suttle, and W. H. Jeffrey. 1998. The role of sunlight in the removal and repair of viruses in the sea. Limnol. Oceanogr. **43:** 586–592.

Wilson, W. H., and N. H. Mann. 1997. Lysogenic and lytic viral production in marine microbial communities. Aquat. Microb. Ecol. **13:** 95–100.

Winget, D. M., K. Williamson, R. Helton, and K. E. Wommack. 2005. Tangential flow dilafiltration: An improved technique for estimation of virioplankton production. Aquat. Microb. Ecol. **41:** 207–216.

———, and K. E. Wommack. 2008. Randomly amplified polymorphic DNA (RAPD)-PCR as a tool for assessment of marine viral richness. Appl. Environ. Microbiol. **74:** 2612–1618.

Winter, C., G. Herndl, and M. G. Weinbauer. 2004a. Diel cycles in viral infection of bacterioplankton in the North Sea. Aquat. Microb. Ecol. **35:** 207–216.

———, A. Smit, G. Herndl, and M. Weinbauer. 2004b. Impact of virioplankton on archaeal and bacterial community richness in seawater batch cultures. Appl. Environ. Microbiol. **70:** 804–813.

———, A. Smit, T. Szoeke-Denes, G. J. Herndl, and M. G. Weinbauer. 2005. Modelling viral impact on bacterioplankton in the North Sea using artificial neural networks. Environ. Microbiol. **7:** 881–893.

Wommack, K. E., and R. R. Colwell. 2000. Virioplankton: Viruses in aquatic ecosystems. Microbiol. Mol. Biol. Rev. **64:** 69–114.

Associate editor: Wade H. Jeffrey

Received: 15 May 2008
Accepted: 22 December 2008
Amended: 08 February 2009